



Contents lists available at ScienceDirect

Science Bulletin

journal homepage: www.elsevier.com/locate/scib

Feature Article

Recent progress on single-molecule nanocatalysis based on single-molecule fluorescence microscopy

Yuwei Zhang^{a,b}, Tao Chen^{a,b,c}, Ping Song^{a,b}, Weilin Xu^{a,b,*}^a State Key Laboratory of Electroanalytical Chemistry, Changchun Institute of Applied Chemistry, Chinese Academy of Sciences, Changchun 130022, China^b Jilin Provincial Key Laboratory of Low Carbon Chemical Power, Changchun Institute of Applied Chemistry, Chinese Academy of Sciences, Changchun 130022, China^c Graduate University of Chinese Academy of Sciences, Beijing 100049, China

ARTICLE INFO

Article history:

Received 2 December 2016

Received in revised form 4 January 2017

Accepted 6 January 2017

Available online xxxx

Keywords:

Single-molecule nanocatalysis

Single-molecule fluorescence microscopy

Activation energy

Electrocatalysis

Super-resolution imaging

ABSTRACT

Understanding the heterogeneous catalytic properties of nanoparticles is of great significance for the development of high efficient nanocatalysts, but the intrinsic heterogeneities of nanocatalysts were always covered in traditional ensemble studies. This issue can be overcome if one can follow the catalysis of individual nanoparticles in real time. This paper mainly summarizes recent developments in single-molecule nanocatalysis at single particle level in Changchun Institute of Applied Chemistry, Chinese Academy of Sciences. These developments include the revealing of catalytic kinetics of different types (plane & edge) of surface atoms on individual Pd nanocubes, the observing of in situ deactivation of individual carbon-supported Pt nanoparticles during the electrocatalytic hydrogen-oxidation reaction, and the measurement of catalytic activation energies on single nanocatalysts for both product formation process and dissociation process, etc. These studies further indicate the advantages or unique abilities of single-molecule methods in the studies of nanocatalysis or even chemical reactions.

© 2017 Science China Press. Published by Elsevier B.V. and Science China Press. All rights reserved.

1. Introduction

Surface reactions on nanocatalysts, including all kinds of catalytic reactions occurring on the solid surfaces, are significantly important for many modern industrial processes, such as fine chemical synthesis, petroleum processing, and energy conversion, etc. [1–8]. Tremendous work had been done with traditional ensemble methods for the understanding of these surface reactions on nanocatalysts [9–11]. Due to heterogeneous properties of nanoparticles in size, shape, morphology or surface composition etc., however, the traditional ensemble methods can not reveal the precise structure-reactivity relationship of the surfaces on nanocatalysts. For a precise understanding of the structure-reactivity relationship of the nanocatalysts, it is highly desirable to study the surface reactions at single-molecule or single-particle level in real time. Recently, the newly-developed technique of single-molecule nanocatalysis based on single-molecule fluorescence microscopy has been proved to be effective for this goal [12–17] and has been used extensively as a new tool to study the catalytic properties of heterogeneous nanocatalysts at single molecule or single particle level [12,18–29].

The single-molecule fluorescence microscopy was initially developed for study of biological systems at single molecule level [30,31]. Later on, this tool was extended to nanocatalysis by counting the individual product molecules formed on single nanocatalysts [21,23,32]. In 2008, based on single-molecule fluorescence microscopy, for the first time, Chen and co-workers [18] studied the catalytic kinetics and dynamics of individual nanocatalysts at the single-molecule single-particle level by monitoring the product formation and dissociation processes on individual nanocatalysts under ambient conditions. In such experiments, the catalytic signal on localized individual nanocatalysts shows stochastic bursts of fluorescence; each burst of fluorescence corresponds to the catalytic formation and dissociation of one product molecule, i.e., one turnover [18] (Fig. 1a, b). From such trajectories, the whole catalytic turnover cycle can be divided into product formation process (t_{off}) and dissociation process (t_{on}). From the statistic analysis of these two parameters, the catalytic kinetics of individual nanocatalysts can be studied.

In this review paper, we summary the recent progress of single-molecule nanocatalysis based on fluorescence microscopy in our group; we also discuss the applications of single molecule fluorescence microscopy in the studies of single molecule/particle redox reactions.

* Corresponding author.

E-mail address: weilinxu@ciac.ac.cn (W. Xu).

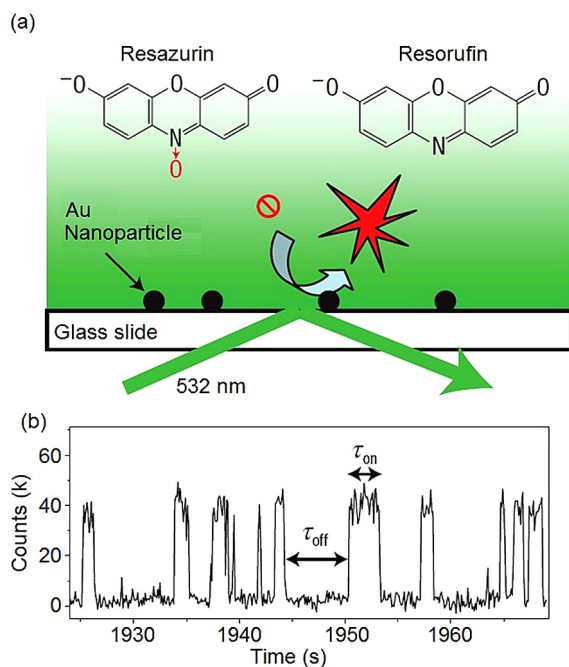


Fig. 1. (Color online) Single-turnover detection of single-Au-nanoparticle catalysis. (a) Experimental design using total internal reflection fluorescence microscopy. (b) A segment of the fluorescence trajectory from the fluorescence spot marked by the arrow in (b) at 0.05 $\mu\text{mol/L}$ Resazurin and 1 mmol/L NH_2OH [18].

2. Single-molecule nanocatalysis

2.1. Revealing the size-dependent catalytic properties and the roles of different types of surface atoms on individual Pd nanocubes

2.1.1. Preparation of flow cell

All the single-molecule fluorescence measurements in our lab mentioned in this paper were based on home-built micro-flow cells, which were fabricated with two pieces of double-sided tapes sandwiched between a quartz slide and a borosilicate coverslip. The 5 min-epoxy was used to seal the interior edges of the tapes. Two holes were drilled on the quartz slides to connect to polyethylene tubings and a syringe pump for reactant continuous solution flow. Before the fabrication of a microflow cell, certain amount of Pd-nanocubes or other nanoparticles in solution were dropped onto one side of the slide. After an incubation period, the side of the slide with particles on was then rinsed with a large amount of water to remove all the unbound nanoparticles.

2.1.2. Single-molecule experiments

Single-molecule fluorescence measurements were performed on a homebuilt prism-type total internal reflection (TIR) fluorescence microscope based on an Olympus IX71 inverted microscope. A continuous wave circularly polarized 532-nm laser beam was focused onto a tiny area on the sample to directly excite the fluorescence of product molecules. The fluorescence of individual product molecules was collected by a 60X NA1.2 water-immersion objective, and projected onto an EMCCD camera. All the single-molecule experiments were carried out within a fresh microflow cell with constant flow rate of reactant solution. In this way, a series of movies were obtained at various substrate Resazurin concentrations. The movies were analyzed to extract the fluorescence intensity trajectories from each localized fluorescence spots by integrating the fluorescence signal counts over an area of $\sim 1 \mu\text{m} \times 1 \mu\text{m}$.

Based on five sets of monodispersed Pd nanocubes (5.2, 7.0, 11.4, 15.2, and 22.2 nm in edge length on average (Fig. 2a–e)) and a simple quantitative deconvolution of product formation rate and dissociation rate obtained from individual nanocatalysts, we studied the catalytic kinetics and dynamics of different surface atoms (plane and edge) quantitatively based on the hydrogenation of Resazurin catalyzed by Pd nanocubes (Fig. 2f, g). The product of this catalytic process is the fluorescent Resorufin, which can be detected individually on localized single nanoparticle surface with single-molecule fluorescence microscopy [33].

Based on statistical single-molecule analysis and two-site Langmuir-Hinshelwood mechanism for the product formation process (Fig. 3a) [33], the product formation rate and dissociation rate on individual nanoparticle were obtained as following:

$$\langle \tau_{\text{off}} \rangle^{-1} = \frac{\gamma_{\text{eff}} a_A [A] a_B [B]}{(1 + a_A [A] + a_B [B])^2}, \quad (1)$$

$$\langle \tau_{\text{on}} \rangle^{-1} = \frac{\gamma_2 G [B] + \gamma_3}{1 + G [B]}, \quad (2)$$

where $[A]$ and $[B]$ are the substrate (A for H_2 , B for Resazurin) concentrations; the rate constant γ_{eff} represents the intrinsic reactivity per nanoparticle; a_A and a_B are the adsorption constants of H_2 and Resazurin on the surface of nanocatalysts; the rate constants of γ_2 and γ_3 are for the indirect and direct dissociation process of product; $G = [A] \gamma_1 / (\gamma_{-1} + \gamma_2)$ is a complex parameter without clear physical meaning.

Firstly, the size-dependence of catalytic kinetics and dynamics of individual Pd nanocubes was studied [34]. As shown in the Fig. 3b, c, the product formation rate and dissociation rate show size-dependent behavior. From these results, we further obtained the kinetic parameters on these Pd nanocubes (Table 1). It shows that the value of γ_{eff} increases with the increase of nanoparticle size. The values of γ_{eff} were further divided by the surface area (S) of single nanoparticles to evaluate the utilization of metal on different nanoparticles. As shown in Table 1, the value of γ_{eff}/S decreases with the size increase inversely, indicating higher metal utilization on smaller nanoparticle or lower catalytic reactivity per catalytic site on larger particles. As for the hydrogen adsorption constant (a_A) on Pd nanoparticles surface (Table 1), it is almost size-independent, probably due to the fast dissociation of H_2 molecule upon adsorption [35]. Whereas the adsorption constant (a_B) of Resazurin increases rapidly with the size increase of Pd nanocubes. In general, the adsorption of adsorbates is usually related to the microenvironment of the adsorption site. The adsorption constants obtained from a whole particle reflects the adsorption ability of adsorbates on the whole surface.

In this work, we also observed the size-dependent selectivity in the product desorption process. As shown in Fig. 3c, the product desorption rate ($\langle \tau_{\text{on}} \rangle^{-1}$) also shows size-dependent desorption behavior. Table 1 shows that small Pd nanocubes show $\gamma_2 < \gamma_3$, indicating the small nanocubes prefer direct desorption pathway; with the size increase, γ_3 decreases gradually to γ_2 , indicating weak desorption selectivity; when the size further increases, such as up to 22.2 nm, γ_3 further decreases and leads to $\gamma_2 > \gamma_3$, indicating that the substrate can promote the product desorption process on large particles.

On the other hand, for a Pd nanocube with size larger than 5 nm [36], the whole surface contains mainly two types of atoms: plane atoms (p) and edge atoms (e) [36,37]. Based on a statistic analysis of surface atoms on face-centered cubic (fcc) nanocrystals [37,38], we obtained the numbers (N_{plane} and N_{edge}) and the fractions ($\chi_p = N_{\text{plane}}/N_s$, $\chi_e = N_{\text{edge}}/N_s$) of different types of surface atoms on a single Pd nanocubes with a particular size. Based on these data, the obtained values of $\langle \tau_{\text{off}} \rangle^{-1}$ and $\langle \tau_{\text{on}} \rangle^{-1}$ (Fig. 3b, c) were

Download English Version:

<https://daneshyari.com/en/article/5788909>

Download Persian Version:

<https://daneshyari.com/article/5788909>

[Daneshyari.com](https://daneshyari.com)